

cGANs with Multi-Hinge Loss

Ilya Kavalero, Wojciech Czaja, Rama Chellappa
 University of Maryland
 ilyak@umiacs.umd.edu

Abstract

We propose a new algorithm to incorporate class conditional information into the discriminator of GANs via a multi-class generalization of the commonly used Hinge loss. Our approach is in contrast to most GAN frameworks in that we train a single classifier for $K + 1$ classes with one loss function, instead of a real/fake discriminator, or a discriminator classifier pair. We show that learning a single good classifier and a single state of the art generator simultaneously is possible in supervised and semi-supervised settings. With our multi-hinge loss modification we were able to improve the state of the art CIFAR10 IS & FID to 9.58 & 6.40, CIFAR100 IS & FID to 14.36 & 13.32, and STL10 IS & FID to 12.16 & 17.44. The code written with PyTorch is available at <https://github.com/ilyakava/BigGAN-PyTorch>.

1. Introduction

Generative Adversarial Networks (GANs) [18] are an attractive approach to constructing generative models that mimic a target distribution, and have shown to be capable of learning to generate high-quality and diverse images directly from data [7]. Conditional GANs [29] (cGANs) are a type of GAN that use conditional information such as class labels to guide the training of the discriminator and the generator. Most frameworks of cGANs either augment a GAN by injecting (embedded) class information into the architecture of the real/fake discriminator [31], or add an auxiliary loss that is class based [36]. We place the class conditional structure at the forefront of the generative model by proposing a loss that ensures generator updates are always class specific. Rather than training a function that measures the information theoretic distance between the generative distribution and one target distribution, we generalize the successful hinge-loss [28] that has become an essential ingredient of many GANs [38, 7] to the multi-class setting and use it to train a single generator classifier pair [38]. While the canonical hinge loss made generator updates according to a class agnostic margin in a real/fake discriminator learned [28], our multi-class hinge-loss GAN updates the generator according to many classification margins. With this modification, we are able to accelerate training and achieve state of the art Inception Scores on CIFAR10, CIFAR100, and STL10.

2. Background

A Generative Adversarial Network [18] is a framework to train a generative model that maps random vectors $z \in \mathcal{Z}$ into data example space $x \in \mathcal{X}$ concurrently with a discriminative network that evaluates its success by judging examples from the dataset and generator as real or fake. The GAN was originally formulated as the minimax game:

$$\begin{aligned} \max_D E_{x \sim p_d} [\log(D(x))] + E_{z \sim p_z} [\log(1 - D(G(z)))], \\ \min_G E_{z \sim p_z} [\log(1 - D(G(z)))], \end{aligned} \tag{1}$$

where p_d is the real data distribution consisting of examples $x \in \mathcal{X}$, p_z is the latent distribution over the latent space \mathcal{Z} , $G : \mathcal{Z} \rightarrow \mathcal{X}$ is the generator neural network, and $D : \mathcal{X} \rightarrow [0, 1]$ is the discriminator neural network. The GAN model transfers the success of the deep discriminative model D to the generative model G and succeeds in generating impressive samples $G(z)$.

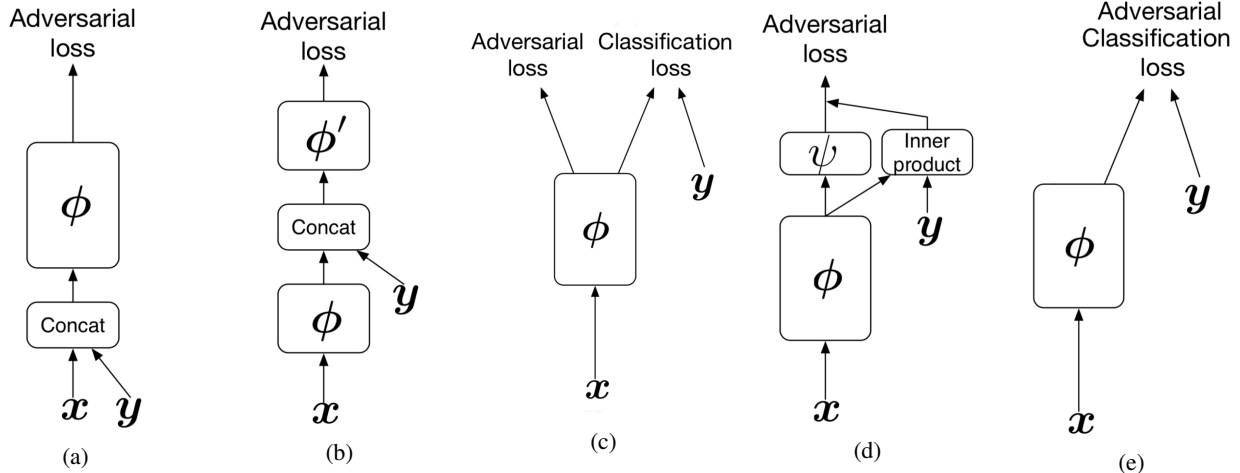


Figure 1: Figure (adapted from [31]) showing architecture differences between cGANs input concat 1a [29] and hidden concat 1b [37], ACGAN 1c [36], projection discriminator GAN 1d [31], and our architecture MHingeGAN 1e.

2.1. Loss Functions for Training GANs

In this paper we will use the word "loss" (and symbol L) for a quantity that we minimize when optimizing. For clarity we rewrite the GAN optimization problem in a more generic form [14] that is amenable to discussion and programming:

$$\begin{aligned} \min_D E_{x \sim p_d} [f(D(x))] + E_{z \sim p_z} [g(D(G(z)))], \\ \min_G E_{z \sim p_z} [h(D(G(z)))]. \end{aligned} \quad (2)$$

Note the two minimums. This is a minor change that will allow us to say that the discriminator seeks to minimize the "discriminator loss," and the generator seeks to minimize the "generator loss." We also don't restrict D to the unit interval but instead $D : \mathcal{X} \rightarrow \mathbb{R}$.

In this case to regain the minimax objective in equation (1) we set $f(w) = \log(1 + e^{-w})$ and $h(w) = -g(w) = -w - \log(1 + e^{-w})$ [14]. [18] showed that this choice minimizes the Jensen-Shannon divergence between p_d and p_g , which denotes the model distribution implicitly defined by $G(z), z \sim p_z$. The minimax objective however was difficult to train, [3] observed that when the discriminator became accurate, that the gradient for the generator vanished.

The study of various ways to measure the divergence or distance between p_d and p_g has been a fruitful source of improved loss functions that make training more stable and samples $G(z)$ of higher quality. [35] showed that the Jensen-Shannon divergence is just one of a family of f-divergences that can be used with success. WGAN [4] found that to minimize the Earth-Mover or Wasserstein-1 distance between p_d and p_g , we should set $f(w) = -w, h(w) = -g(w) = -w$ and clip the weights of D . This setting greatly improved the ease and quality of training and reduced the mode dropping problem of GANs. In [32] the Wasserstein-1 distance was shown to be a special instance of minimizing the integral probability metric (IPM) between p_d and p_g . [32] introduced a mean and covariance feature matching IPM loss (McGAN) following the empirical successes of the Maximum Mean Discrepancy objective [27] and feature matching [38].

The mean feature matching of McGAN has a geometric interpretation as well, [28] found that the gradient updates of feature matching for generator updates are normal to the separating hyperplane learned by the discriminator. [28] also found that using the SVM like hinge-loss choice of $f(w) = \max(0, 1 - w), g(w) = \max(0, 1 + w)$ and $h(w) = -w$ [28, 41] the gradient updates would be similar to those of McGAN. When combined with spectral normalization of weights in D [30], the hinge loss greatly improves performance, and has become a mainstay in recent state of the art GANs [7, 45, 31]. In this work we generalize this hinge loss to a multi-class setting. Some additional choices for f, g, h and their consequences are summarized in [14].

2.2. Supervised Training for Conditional GANs

Conditional GANs (cGANs) are a type of GAN that use conditional information [29] in the discriminator and generator. G and D become functions of the pairs $(z \sim p_z, y \sim p_d)$ and $(x, y) \sim p_d$, where y is the conditional data, for example the

class labels of an image. For example, in a cGAN with a hinge loss, the discriminator would minimize L_D in [equation \(3\)](#), and the generator would minimize L_G in [equation \(3\)](#), as in [\[45, 7\]](#).

$$\begin{aligned}
L_D &= E_{(x,y) \sim p_d} [\max(0, 1 - D(x, y))] \\
&\quad + E_{z \sim p_z, y \sim p_d} [\max(0, 1 + D(G(z, y), y))] \\
&= L_{D_{\text{real}}} + L_{D_{\text{fake}}}, \\
L_G &= - E_{z \sim p_z, y \sim p_d} [D(G(z, y), y)].
\end{aligned} \tag{3}$$

We briefly review some relevant work on using conditional information to train the discriminator of GANs, as well as uses of classifiers.

In the discriminator many approaches use class labels to add more structure in the latent space by concatenating (embedded) labels $y \sim p_d$ to the input [\[29\]](#) or at some intermediate feature vector in the discriminator [\[13, 37, 15\]](#). A projection discriminator [\[31\]](#) is a type of conditional discriminator that adds the inner product between an intermediate feature and a class embedding to its final output, and proves highly effective when combined with spectral normalization in G [\[31, 45, 7\]](#). Using multiple discriminator networks [\[33, 17\]](#) or multiple sub-networks of a single discriminator [\[34\]](#) has also been explored.

Several GANs have used a classifier in addition to or in place of a discriminator to improve training. CatGAN [\[40\]](#) replaces the discriminator with a K class classifier trained with cross entropy loss that the generator tries to confuse. ALI [\[15\]](#) trains an encoder decoder pair with a discriminator, while also using the encoder for inference in a semi-supervised setting. ACGAN [\[36\]](#) uses an auxiliary classification network or extra classification layer appended to the discriminator, and adds the cross entropy loss from this network to the minimax GAN loss. Triple GAN [\[8\]](#) trains a classifier in addition to a discriminator and updates it with a special minimax type loss.

Most relevant to this work is the Improved GAN [\[38\]](#) $K + 1$ classifier originally proposed for semi-supervised learning with feature matching loss. The single conditional critic architecture of $D : (x, y) \rightarrow \mathbb{R}$ is swapped for the classifier architecture $C : x \rightarrow \mathbb{R}^{K+1}$ where there are K class labels and an extra label for fake images (the "+1") [\[38\]](#). The Improved GAN trains this classifier architecture in a semi-supervised setting with log-likelihood loss, and trains the generator with the mean feature matching loss. This work uses the Improved GAN $K + 1$ classifier but instead alters the class agnostic feature matching loss used there with class specific multi-hinge loss terms. BadGAN [\[11\]](#) used the Improved GAN to achieve state of the art performance on semi-supervised learning and found in their setting that the aim of having a low classification error on the K real classes is orthogonal to generating realistic examples.

3. Multi-Hinge Loss

We propose a multi-hinge loss as a competitive alternative to projection discrimination [\[31\]](#), the current state of the art in cGANs. Our formulation uses the $K + 1$ classifier architecture of [\[38\]](#), but instead of using cross entropy to train this fake v.s. real $_k, k = 1, \dots, K$ classifier, we generalize the binary hinge loss [\[28, 41\]](#) to a multi-class hinge loss known for SVMs [\[10\]](#), and use it to train a spectrally normalized WGAN [\[4, 20, 30\]](#).

We denote the classifier architecture [\[38\]](#) as $C : x \rightarrow \mathbb{R}^{K+1}$ where the class labels are $y \in \{1, \dots, K\}$ and the label for fake images is 0. We let $C_k(x)$ denote the k th element of the vector output of C for an example x , which represents the affinity of class k for x . The multi-hinge loss for the classifier L_C is:

$$\begin{aligned}
L_C &= E_{(x,y) \sim p_d} [\max(0, 1 - C_y(x) + C_{-y}(x))] \\
&\quad + E_{z \sim p_z, y \sim p_d} [\max(0, 1 + C_{-0}(G(z, y)) - C_0(G(z, y)))] \\
&= L_{C_{\text{real}}} + L_{C_{\text{real}}},
\end{aligned} \tag{4}$$

where $C_{-y}(x)$ is the classifier's highest affinity for any label that is "not y ": $C_{-y}(x) = \max_{k \neq y} C_k(x), y = 0, 1, \dots, K$.

For the generator, we find the best performance when pairing the class specific multi-hinge loss with a class agnostic feature matching loss, as will be discussed in [Section 3.2](#):

$$\begin{aligned}
L_{G,\lambda} &= \lambda E_{z \sim p_z, y \sim p_d} [\max(0, 1 - C_{-y}(G(z, y)) + C_y(G(z, y)))] \\
&\quad + \|E_{z \sim p_z, y \sim p_d} [C_{\text{feat}}(G(z, y))] - E_{x \sim p_d} [C_{\text{feat}}(x)]\|_1 \\
&= \lambda L_{G,CS} + L_{G,FM},
\end{aligned} \tag{5}$$

The advantage of training a classifier and generator trained with L_C in [equation \(4\)](#) and $L_{G,\lambda}$ in [equation \(5\)](#) is the main result of our paper. In the following sections we discuss the motivation for each of these components, and mention what happens when we train the generator without the class specific term $L_{G,CS}$.

3.1. Motivation behind the Multi-Hinge Loss

In this section we describe the motivation for L_C in [equation \(4\)](#). A class conditional discriminator should obviously not output "real" when it is conditioned on the wrong class. That is for a pair $(x, y) \sim p_d$ we expect if our discriminator loss is minimized then so is the quantity: $1 - D(x, y) + D(x, k), k \neq y$ (recall that in WGANs D is not a probability measure and may take values outside $[0, 1]$). This quantity is positive for all k so long as the output of the discriminator conditioned on the correct label is larger by at least one than the discriminator conditioned on the rest of the labels. To explicitly enforce this margin, we could minimize the expectation:

$$L_{D_{\text{real}}} = E_{(x,y) \sim p_d} [\max(0, 1 - D(x, y) + \max_{k \neq y} D(x, k))] \tag{6}$$

This form of a hinge-loss has been used by [\[10\]](#) in their formulation of efficient multi-class kernel SVMs. For this loss to be minimized the discriminator must always have an affinity for the correct label y by a margin of 1 over the incorrect labels $k \neq y$. The function inside the ReLU can be thought of as: one minus the affinity for the target label plus the affinity for the maximum wrong label. The ReLU $\max(0, \cdot)$ leads [equation \(6\)](#) to ignore cases where the correct decision is made with a margin more than 1. A clear downside of the loss in [equation \(6\)](#) compared to $L_{D_{\text{real}}}$ in [equation \(3\)](#) is that it takes K times more operations to compute, however there is a simple way to avoid this extra computation.

Instead of training the generator with a single conditional critic architecture of $D : (x, y) \rightarrow \mathbb{R}$ we use a single classifier architecture $C : x \rightarrow \mathbb{R}^{K+1}$ where the class labels are $y \in \{1, \dots, K\}$ and the label for fake images is 0 [\[38\]](#). A single evaluation of $C(x)$ replaces K of $D(x, k)$. For real data $(x, y) \sim p_d$ we then enforce the margin between $C(x)$'s affinity for class y and its affinity for not class y . That is we minimize the expectation:

$$L_{C_{\text{real}}} = E_{(x,y) \sim p_d} [\max(0, 1 - C_y(x) + C_{-y}(x))]. \tag{7}$$

$L_{C_{\text{real}}}$ builds in class discriminability into the GAN training process.

Similarly, when we generate fake data from $z \sim p_z, y \sim p_d$ we train our classifier to enforce the margin between the fake class and all the real classes by minimizing the expectation:

$$L_{C_{\text{fake}}} = E_{z \sim p_z, y \sim p_d} [\max(0, 1 + C_{-0}(G(z, y)) - C_0(G(z, y)))]. \tag{8}$$

Thus $L_C = L_{C_{\text{real}}} + L_{C_{\text{fake}}}$ of [equation \(4\)](#) becomes our multi-hinge loss for the classifier.

A typical cGAN with hinge-loss will train its discriminator and generator to gradients orthogonal to a single real/fake margin [\[28\]](#). The multi-hinge Crammer-Singer loss we use with a classifier allows training the discriminator in a class specific way. This constraining choice acts as a regularizer on the discrimination aim of the GAN pair. In [section 4.2](#) we show that this modification does indeed retain more conditional information in the discriminator/classifier of the GAN.

3.2. Generator Loss

For training the generator we find it is advantageous to not constrain it as strictly as the classifier, but to use both class specific and class agnostic updates.

Class Agnostic Loss Choices. We find that class agnostic losses can even be used by themselves with no class specific term to train a competitive generator. We compare the performance of two class agnostic losses, a feature matching loss, and the "complement" of the Crammer-Singer multi-hinge loss. The well known mean feature matching loss [\[38, 32\]](#) we use to train the generator is:

$$L_{G,FM} = \|E_{z \sim p_z, y \sim p_d} [C_{\text{feat}}(G(z, y)) - E_{x \sim p_d} [C_{\text{feat}}(x)]]\|_1, \tag{9}$$

where C_{feat} denotes the features before the final classification layer of C . When used with real/fake discriminators this loss has an interpretation of updating the G such that it generates examples on the wrong side of D 's discrimination hyperplane [\[28\]](#). The corresponding interpretation here would be that the generator is updated to generate examples on the wrong side

of a hyperplane obtained from averaging the K class specific hyperplanes of C . This loss can be computed with labelled or unlabelled examples alike from the real data distribution.

We find that a successful multi-hinge form loss is the complement of the Crammer-Singer loss $L_{C_{\text{fake}}}$, that is:

$$L_{G,CSC} = E_{z \sim p_z, y \sim p_d} [\max(0, 1 - C_{-0}(G(z, y)) + C_0(G(z, y)))], \quad (10)$$

This Crammer-Singer Complement (CSC) form ensures that the margin is at least 1 between at least one real class and the fake class. A generator trained only with $L_{G,CSC}$ performs similarly to a generator trained only with $L_{G,FM}$.

Class Specific Loss. Through experimentation we find the above relaxed class agnostic losses are easier to train alone than several others that could be more specific; i.e. bounding the margin between the fake class and all real classes, or between the fake class the correct y label class. However, adding a class specific loss with a small weight proved to be advantageous. For this aim we use the same Crammer-Singer type loss that is used in the discriminator, and pair it with the feature matching loss. Hence we set the loss for G to be [equation \(5\)](#). λ is a hyperparameter that balances how much class specificity should be incorporated. In practice, if set too high then training collapses early, if set too low, then the generator never learns to use its conditioning information.

3.3. Semi-Supervised Learning

When additional unlabeled data $x \sim p_{\text{unlab}}$ is available, we modify the classifier loss L_C and the feature matching loss in the generator slightly. For the classifier we add a single term:

$$\begin{aligned} L_C = & E_{(x,y) \sim p_d} [\max(0, 1 - C_y(x) + C_{-y}(x))] \\ & + E_{z \sim p_z, y \sim p_d} [\max(0, 1 + C_{-0}(G(z, y)) - C_0(G(z, y)))] \\ & + E_{x \sim p_{\text{unlab}}} [\max(0, 1 - C_{-0}(x) + C_0(x)), \end{aligned} \quad (11)$$

and for the feature matching loss, we instead calculate the mean feature over the unlabeled data:

$$L_{G,FM} = \|E_{z \sim p_z, y \sim p_d} [C_{\text{feat}}(G(z, y))] - E_{x \sim p_{\text{unlab}}} [C_{\text{feat}}(x)]\|_1. \quad (12)$$

4. Experiments

As our baseline, we use the most basic BigGAN architecture [7] and add our loss implementations on top of the BigGAN-PyTorch implementation [6]. The BigGAN baseline was chosen for its exceptional performance demonstrated in [7]. We also tried our improvements to the conditional variant of the SNGAN [30] architecture which is like ACGAN; improvements in IS were much more visible here, but still below the number reported by BigGAN. The BigGAN we use as a baseline is the ResNet [21] GAN architecture [45, 31, 30] adapted for 32x32 and 48x48 resolutions, architecture details are in [Section B](#). Conditional information is given to G using class conditional BatchNorm [16, 12] and to D with projection discrimination [31]. We train with the hinge loss [28, 41] in [equation \(3\)](#). Spectral norm is applied to both D and G [45, 31]. For size 32 images the optimization settings follow [6]: we use size 50 batches, learning rates of $2e - 4$ and take 4 D steps per G step, and normalize the weights as $\mathcal{N}(0, 0.02I)$. For size 48 images we use the optimization settings in [7, 6] with size 128 batches, learning rates of $1e - 4$ and $4e - 4$ for G and D and 2 D steps per G step, and use orthogonal initialization. We use EMA to average the weights of G with a decay of 0.9999 [7]. Features of BigGAN that we leave out attention layers [45], shared embeddings, skip-z connections, and orthogonal regularization. We use 64 channels and limit most of our experiments to 100,000 iterations. To this baseline we compare the performance of the following models:

MHingeGAN. We train a single $K + 1$ classifier and generator pair and use the loss in [equation \(4\)](#) to train C and the loss in [equation \(5\)](#) to train G . To do this we replace the final discriminator layer in the baseline’s D with a classification layer and do not use any form of projection discriminator, i.e. C does not use y as an input. We set $\lambda = 0.05$ for this paper. This setting was chosen by training on CIFAR100: it was the highest $\lambda \in \{0.01, 0.05, 0.1, 0.25, 0.5, 1.0\}$ that did not lead to early collapse.

MHingeGAN SSL. To incorporate the use of unlabelled data in a semi-supervised setting, we add a single term to C ’s loss in MHingeGAN like in [equation \(11\)](#). We train G including the change in [equation \(12\)](#). $\lambda = 0.05$ for this model too.

These are our two best models. We also present results on some ablations of these two models:

MHingeGAN FM. This is simply MHingeGAN with λ set to 0.

MHingeGAN CSC. This is MHingeGAN but with G trained via [equation \(10\)](#).

MHingeGAN FM SSL. This is MHingeGAN FM with the SSL changes in [equations \(11\)](#) and [\(12\)](#).

MHingeGAN CSC SSL. This is MHingeGAN SSL but with G trained via [equation \(10\)](#).

The key difference between the baseline BigGAN and the MHingeGANs is that the projection discriminator has been removed, and in its place a $K + 1$ class classifier [38] is trained with one of the losses detailed above. The key difference between MHingeGAN (SSL) and the ablations/alterations of it is that class specific training is done on the generator.

We use the Inception score (IS) [38] and Frechet Inception Distance (FID) for quantitative evaluation of our generative models. We compute both over 10 independent groups of 5,000 randomly generated samples using the official tensorflow implementations [1].

Table 1: Inception Scores and FIDs for supervised image generation. Each row corresponds to a single trained model. The models we trained were chosen by minimizing the IS within 100,000 iterations. Methods that are not class conditional are indicated by the †. The best number per column is bold faced.

Method	CIFAR10		Method	CIFAR100	
	IS	FID		IS	FID
Real data	11.23 (\pm .20)		Real data	14.79 (\pm .18)	
Baseline	9.07 (\pm .13)	8.47	Baseline	10.88 (\pm .19)	11.53
MHingeGAN	9.58 (\pm .09)	7.50	MHingeGAN	14.36 (\pm .17)	17.3
MHingeGAN CSC	9.35 (\pm .12)	15.11	MHingeGAN CSC	8.79 (\pm .08)	21.03
MHingeGAN FM	7.42 (\pm .08)	34.10	MHingeGAN FM	7.86 (\pm .03)	31.55
BigGAN [7]	9.22	14.73	SNGAN [39]	9.30 (\pm .08)	15.6
CA-GAN [34]	9.17 (\pm .13)	-	MSGAN† [42]	-	19.74
Splitting GAN [19]	8.87 (\pm .09)	-			
CR-GAN [2]	8.40	11.67			
SVD GAN [23]	8.21 (\pm .05)	19.5			

4.1. Fully Supervised Image Generation

We present results on MHingeGAN on the CIFAR10 dataset and the CIFAR100 dataset [25, 24] in a fully supervised manner. CIFAR10 contains 50,000 labeled training images of size 32x32 with 10 classes. CIFAR100 contains 50,000 labeled training images of size 32x32 with 100 classes. Performance comparisons to our baseline are in [Table 1](#). Of the two class agnostic models, MHingeGAN CSC outperformed MHingeGAN FM.

On CIFAR10, we beat the previous state of the art BigGAN with our model which has a much smaller batch size and surpasses an IS of 9.22 by 25,000 steps (which takes only 5.3 hours on a single GeForce GTX TITAN X). On CIFAR100, our best IS comes just 0.43 below the presumed limit (the IS of the real data). If we were to choose our best models by minimizing FID, they would be (9.53 \pm .14, 6.40) for CIFAR10, and (12.60 \pm .16, 13.32) for CIFAR100 (IS,FID). Our two class agnostic models show that class specificity is more important when more classes are present, as we discuss in the next section.

4.2. Measuring the conditioning of the Discriminator and Generator

We attribute our model’s success from the fact that it incorporates more class specific information into both the discriminator/classifier and the generator than projection discrimination. The way we measure this information was introduced in [Section 3.1](#) and is expanded here.

When we have a classifier like with MHingeGAN, it is straightforward to calculate the following four accuracies:

1. **Train:** The classifier predicts the label of real training data. We estimate this accuracy from 10k random examples. This measures how well the information in the training data has been absorbed and therefore training progress.
2. **Test:** The classifier predicts the label of real testing data, the whole standard testing partition of the dataset is used. This measures how good the classifier learned is, and at what point it starts to overfit.

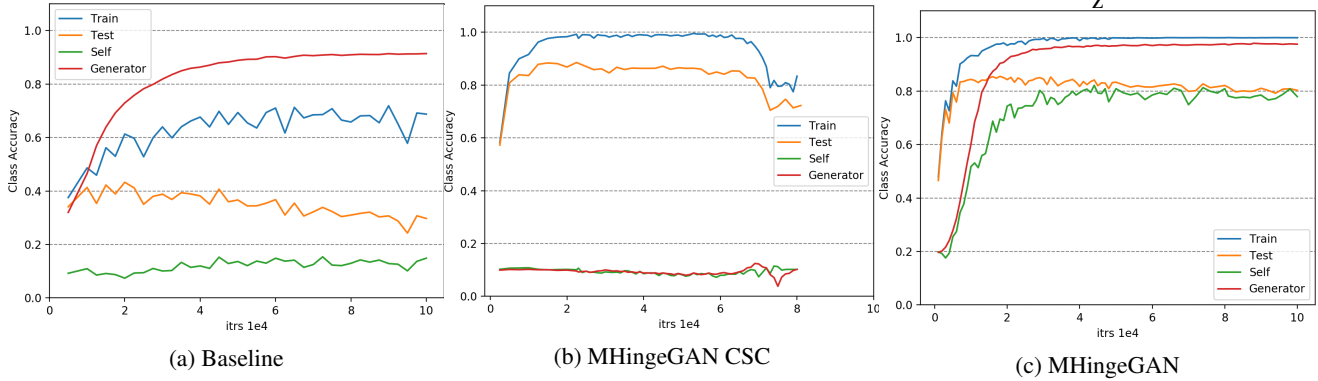


Figure 2: The four accuracies of Section 4.2 for CIFAR10 for 3 models. MHingeGAN CSC collapsed around 71k iterations.

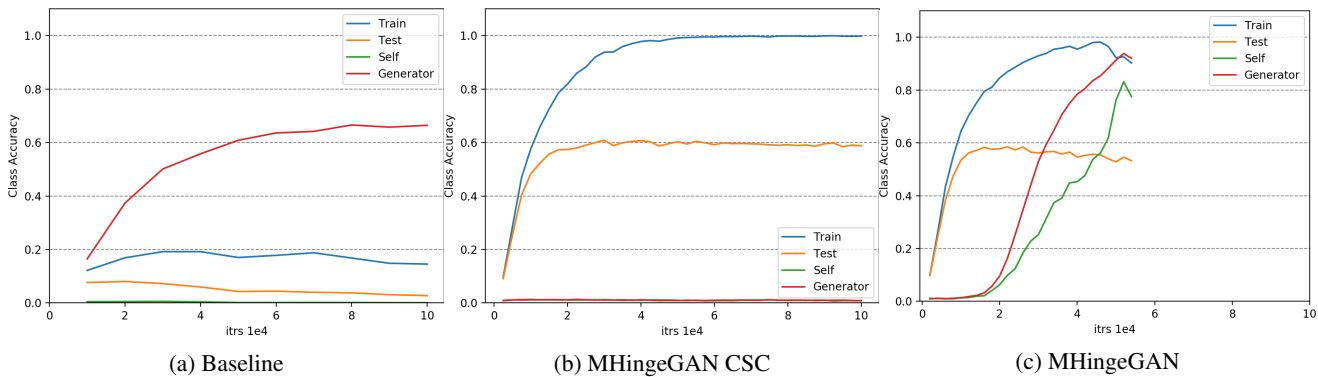


Figure 3: The four accuracies of Section 4.2 for CIFAR100 for 3 models. MHingeGAN collapsed around 58k iterations.

3. **Self:** We see if $\arg \max_{k=1, \dots, K} C_k(G(z, y))$ equals y . This measures how G incorporates the label information into its output, as measured by our concurrently trained C. This measure self consistency.
4. **Generator:** We see if $\mathcal{C}(G(z, y))$ equals y where \mathcal{C} is a separately trained classifier on the training data (details in Section D). We include this measure to again see how well G incorporates the label information into its output, as measured by a more accurate network. The motivation to include this measure is driven more by our baseline BigGAN, whose discriminator does not discriminate class labels well but whose generator clearly respects its conditioning. This accuracy is meant to purely measure G’s use of the conditional information.

To compute class accuracies the fake class in the $K + 1$ classifier is always ignored, and the max over the real classes is taken. For the baseline network with a projection discriminator, to perform classification we use the method mentioned in Section 3.1. That is our “classification” for an example x is $\arg \max_{k=1, \dots, K} D(x, k)$, where each k is used as input to the projection discriminator layer that was trained.

Conditional Information in C&D. We find that our suspicion from Section 3.1 is confirmed for the baseline projection discriminator model: for $(x, y) \sim p_d$ it is not the case that $D(x, y) > D(x, k), k \neq y$ with high probability. This tells us that the projection discriminator has not learned all the information given to it in the training data. We find that using the multi-hinge loss indeed trains a better classifier than projection discrimination with a regular hinge loss, and that $C_y(x) > C_k(x), k \neq y$ with relatively high probability. For CIFAR10, we see that the train accuracy goes to 100% for the MHingeGAN models in Figures 2b and 2c, but not for the projection discriminator baseline Figure 2a. The situation is even more dramatic for CIFAR100, the projection discriminator is maximally activated for the correct class on training data at most 20% of the time, while both MHingeGAN and MHingeGAN CSC approach 100%. On test data, the baseline only classifies 2-4x better than random, while MHingeGAN does 60x better than random on CIFAR100. We don’t see any drastic overfitting in the models, though the test accuracy does decrease slightly. From these charts we can say that less class information is stored in the baseline’s D versus the MHingeGAN’s C, as expected. Similar charts for STL10 are in Section E.

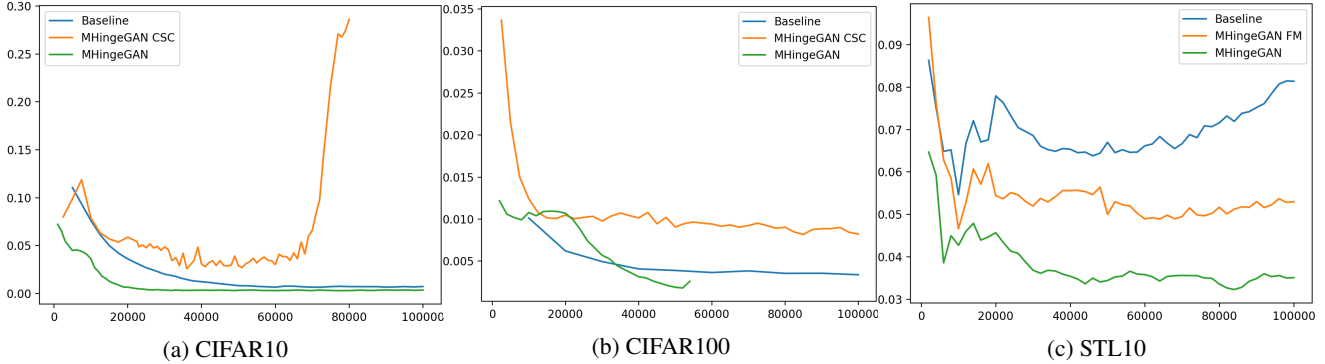


Figure 4: The standard deviation of class prevalences (see Section 4.2) for 3 models per the 3 datasets we evaluate on. A std. dev. of 0 would mean that the generator produces samples with the same uniform distribution of the class label $y \sim p_d$ fed to it; that $\mathcal{C}(G(z, y)) = y$ always.

Conditional Information in G. In Figure 2b and Figure 3b we notice that the self and generator accuracies are near random for MHingeGAN CSC, indicating that the labels given to the generator in the class agnostic MHingeGAN CSC are not respected. Curiously, we could conclude from these charts that the generator of MHingeGAN CSC is not conditional (in the sense that it disregards its conditioning) even though the classifier clearly is. To take a closer look at this point, we introduce the concept of the mean and standard deviation of class prevalence.

When we calculated the generator accuracies in Figures 2 and 3 and for STL with an auxiliary network \mathcal{C} , we also recorded the prevalence of each of the classes according to \mathcal{C} . To measure the prevalence of a class k for a generator we generated 10,000 samples and calculated the fraction of the 10,000 that \mathcal{C} classified as k . If our uniform prior over $y \sim p_d$ were to be completely respected by the examples generated, then we would expect the mean class prevalence to be $1/10$ for CIFAR10 and $1/100$ for CIFAR100, with a standard deviation of zero. In this case a conditional generator would use the label it was conditioned on 100% accurately. If some classes were overproduced by the generator and others were underproduced, then this standard deviation would be non-zero. In the case of an unconditionally trained generator (like our baseline for STL10), there would be no reason to expect that the prior over labels the generator learned would be perfectly uniform. We show the standard deviation over class prevalences for our models in Figure 4. In Figures 4a and 4b we see that the baseline has a lower std. dev. than MHingeGAN CSC, and MHingeGAN has a lower std. dev. than the baseline. A higher class prevalence std. dev. means class imbalances in the outputs of the generator, which we see hurts the IS and FID of MHingeGAN CSC in Table 1. Qualitatively we notice the class imbalance leads to the class agnostic generators preferring to generate more simple "blob" like objects and neglecting more complicated objects like dogs.

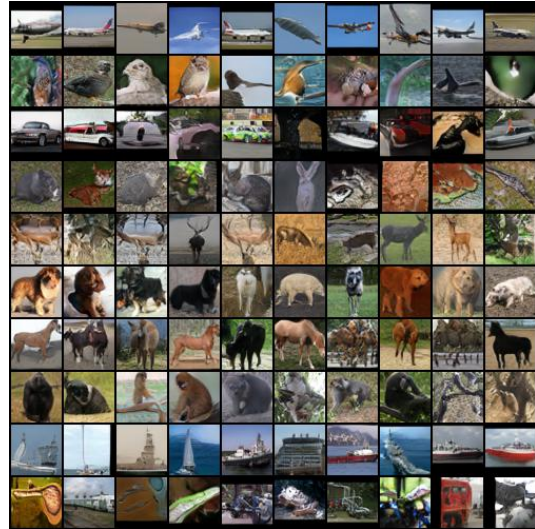
We see in Figure 4 that the class prevalence std. dev. is consistently lowest for MHingeGAN, and that both the self and generator accuracies are highest for MHingeGAN in Figures 2 and 3. Both of these factors are likely important for the exceptional IS and FID scores for MHingeGAN in Table 1. MHingeGAN having the lowest class prevalence std. dev. and the highest generator accuracy indicates that the generator of MHingeGAN respects the conditional information input into it more than the projection discriminator baseline. The higher self accuracy means that MHingeGAN's classifier/discriminator sees the conditional information of the generator better.

4.3. Semi-Supervised Image Generation

STL10 [9] is a subset from ImageNet which is more diverse than CIFAR10. It contains 105,000 images of size 96x96, 5,000 of which have class labels. We rescale the STL10 images down to 48x48 (the appendix contains some results on 32x32 STL10 images). We use this dataset in a semi-supervised way using both labeled and unlabeled images and train MHingeGANs as described in Section 3.3. For our baseline, we tried training projection discrimination in a semi-supervised manner by bypassing the projection layer when the conditioning label y was not present, but this led to collapse. Therefore our baseline was an unconditional discriminator for the STL experiments. Because of this, we could not make the train/test/self accuracy plots for the baseline generator we trained, but the four accuracies for two MHGANs are in Section E. The standard deviation of the prevalences are in Figure 4c. We see that the highest std. dev. is in the fully unconditional baseline model, followed by the class agnostically trained MHingeGAN FM, and the class specific training of the MHingeGAN yields the lowest std. dev.

Table 2: Inception Scores and FIDs for supervised image generation. Each row corresponds to a single trained model. The models we trained were chosen by minimizing the IS within 100,000 iterations. The best number per column is bold faced. The images are randomly sampled from the bolded model. The classes are: Airplane, bird, car, cat, deer, dog, horse, monkey, ship, truck.

Method	STL10 48x48	
	IS	FID
Real data	24.57 (\pm .38)	
Baseline [†]	9.85 (\pm .12)	33.16
MHingeGAN SSL	12.16 (\pm .14)	17.59
MHingeGAN CSC SSL	9.76 (\pm .16)	30.58
MHingeGAN FM SSL	10.78 (\pm .12)	31.48
CA-GAN [2]	10.02 (\pm .13)	-
Splitting GAN [†] [19]	9.50 (\pm .13)	-
SVD GAN [23]	9.65 (\pm .06)	39.9



Compared to other methods, our MHingeGAN yields a higher IS and a lower FID. If we were to choose our best model by minimizing FID, it would be an IS of $12.12 \pm .17$ with an FID of 17.44. We do notice that unlike at the resolution of 32x32, between the two class agnostic losses FM works better than CSC loss, this could perhaps be due to the deeper 48x48 network used for D/C leading to more semantic features. We did verify it was not because of the increased batch size.

5. Conclusion

We find MHingeGAN to be a powerful alternative to projection discrimination, and show that MHingeGAN retains more class specific information than projection discrimination in Section 4.2. Tables 1 and 2 show state of the art performance of MHingeGAN on the CIFAR10 and CIFAR100 datasets, and MHingeGAN SSL on the STL10 dataset. The class specific loss on the generator is shown to be essential for superior performance, and stores more conditional information in the discriminator/classifier and the generator. The class specificity of MHingeGAN stands out in the 100 class case especially. MHingeGAN is able to perform well in both fully supervised and semi-supervised settings, and learns an accurate classifier concurrently with a high quality generator.

References

- [1] bioinf-jku/TTUR, Nov. 2019. original-date: 2017-06-26T13:32:12Z. 6
- [2] Anonymous. Consistency regularization for generative adversarial networks. In *Submitted to International Conference on Learning Representations*, 2020. under review. 6, 9
- [3] Martin Arjovsky and Lon Bottou. Towards Principled Methods for Training Generative Adversarial Networks. In *International Conference on Learning Representations*, 2017. 2
- [4] Martin Arjovsky, Soumith Chintala, and Lon Bottou. Wasserstein GAN. *arXiv:1701.07875 [cs, stat]*, Dec. 2017. arXiv: 1701.07875. 2, 3
- [5] David Berthelot, Nicholas Carlini, Ian Goodfellow, Nicolas Papernot, Avital Oliver, and Colin A Raffel. Mixmatch: A holistic approach to semi-supervised learning. In H. Wallach, H. Larochelle, A. Beygelzimer, F. d’Alché Buc, E. Fox, and R. Garnett, editors, *Advances in Neural Information Processing Systems 32*, pages 5050–5060. Curran Associates, Inc., 2019. 14
- [6] Andy Brock. ajbrock/BigGAN-PyTorch, Nov. 2019. original-date: 2019-01-20T18:50:49Z. 5
- [7] Andrew Brock, Jeff Donahue, and Karen Simonyan. Large scale GAN training for high fidelity natural image synthesis. In *International Conference on Learning Representations*, 2019. 1, 2, 3, 5, 6
- [8] LI Chongxuan, Taufik Xu, Jun Zhu, and Bo Zhang. Triple generative adversarial nets. In *Advances in neural information processing systems*, pages 4088–4098, 2017. 3

- [9] Adam Coates, Andrew Ng, and Honglak Lee. An analysis of single-layer networks in unsupervised feature learning. In Geoffrey Gordon, David Dunson, and Miroslav Dudk, editors, *Proceedings of the Fourteenth International Conference on Artificial Intelligence and Statistics*, volume 15 of *Proceedings of Machine Learning Research*, pages 215–223, Fort Lauderdale, FL, USA, 11–13 Apr 2011. PMLR. 8
- [10] Koby Crammer and Yoram Singer. On the algorithmic implementation of multiclass kernel-based vector machines. *Journal of machine learning research*, 2(Dec):265–292, 2001. 3, 4
- [11] Zihang Dai, Zhilin Yang, Fan Yang, William W Cohen, and Russ R Salakhutdinov. Good semi-supervised learning that requires a bad gan. In *Advances in neural information processing systems*, pages 6510–6520, 2017. 3
- [12] Harm De Vries, Florian Strub, Jérémie Mary, Hugo Larochelle, Olivier Pietquin, and Aaron C Courville. Modulating early visual processing by language. In *Advances in Neural Information Processing Systems*, pages 6594–6604, 2017. 5
- [13] Emily Denton, Soumith Chintala, Arthur Szlam, and Rob Fergus. Deep generative image models using a laplacian pyramid of adversarial networks. In *Proceedings of the 28th International Conference on Neural Information Processing Systems - Volume 1*, NIPS’15, pages 1486–1494, Cambridge, MA, USA, 2015. MIT Press. 3
- [14] Hao-Wen Dong and Yi-Hsuan Yang. Towards a Deeper Understanding of Adversarial Losses. *arXiv:1901.08753 [cs, stat]*, Jan. 2019. arXiv: 1901.08753. 2
- [15] Vincent Dumoulin, Ishmael Belghazi, Ben Poole, Alex Lamb, Martin Arjovsky, Olivier Mastropietro, and Aaron Courville. Adversarially Learned Inference. In *International Conference on Learning Representations*, 2017. 3
- [16] Vincent Dumoulin, Jonathon Shlens, and Manjunath Kudlur. A Learned Representation For Artistic Style. In *International Conference on Learning Representations*, 2017. 5
- [17] Ishan Durugkar, Ian Gemp, and Sridhar Mahadevan. Generative Multi-Adversarial Networks. In *International Conference on Learning Representations*, 2017. 3
- [18] Ian J Goodfellow, Jean Pouget-Abadie, Mehdi Mirza, Bing Xu, David Warde-Farley, Sherjil Ozair, Aaron Courville, and Yoshua Bengio. Generative adversarial nets. In *Proceedings of the 27th International Conference on Neural Information Processing Systems - Volume 2*, pages 2672–2680. MIT Press, 2014. 1, 2
- [19] Guillermo L. Grinblat, Lucas C. Uzal, and Pablo M. Granitto. Class-Splitting Generative Adversarial Networks. *arXiv:1709.07359 [cs, stat]*, May 2018. arXiv: 1709.07359 version: 2. 6, 9
- [20] Ishaan Gulrajani, Faruk Ahmed, Martin Arjovsky, Vincent Dumoulin, and Aaron C Courville. Improved training of wasserstein gans. In *Advances in neural information processing systems*, pages 5767–5777, 2017. 3
- [21] Kai Ming He, Xiangyu Zhang, Shaoqing Ren, and Jian Sun. Deep residual learning for image recognition. In *Proceedings of the IEEE conference on computer vision and pattern recognition*, pages 770–778, 2016. 5
- [22] Gao Huang, Zhuang Liu, Laurens van der Maaten, and Kilian Q. Weinberger. Densely Connected Convolutional Networks. In *2017 IEEE Conference on Computer Vision and Pattern Recognition (CVPR)*, pages 2261–2269, Honolulu, HI, July 2017. IEEE. 14
- [23] Haoming Jiang, Zhehui Chen, Minshuo Chen, Feng Liu, Dingding Wang, and Tuo Zhao. On computation and generalization of generative adversarial networks under spectrum control. In *International Conference on Learning Representations*, 2019. 6, 9
- [24] Alex Krizhevsky et al. Learning multiple layers of features from tiny images. Technical report, Citeseer, 2009. 6
- [25] Alex Krizhevsky, Vinod Nair, and Geoffrey Hinton. Cifar-10 (canadian institute for advanced research). 6
- [26] kuangliu. kuangliu/pytorch-cifar, Dec. 2019. original-date: 2017-01-21T05:43:20Z. 14
- [27] Chun-Liang Li, Wei-Cheng Chang, Yu Cheng, Yiming Yang, and Barnabás Póczos. Mmd gan: Towards deeper understanding of moment matching network. In *Advances in Neural Information Processing Systems*, pages 2203–2213, 2017. 2
- [28] Jae Hyun Lim and Jong Chul Ye. Geometric GAN. *arXiv:1705.02894 [cond-mat, stat]*, May 2017. arXiv: 1705.02894. 1, 2, 3, 4, 5
- [29] Mehdi Mirza and Simon Osindero. Conditional Generative Adversarial Nets. *arXiv:1411.1784 [cs, stat]*, Nov. 2014. arXiv: 1411.1784. 1, 2, 3
- [30] Takeru Miyato, Toshiki Kataoka, Masanori Koyama, and Yuichi Yoshida. Spectral normalization for generative adversarial networks. In *International Conference on Learning Representations*, 2018. 2, 3, 5, 12
- [31] Takeru Miyato and Masanori Koyama. cGANs with projection discriminator. In *International Conference on Learning Representations*, 2018. 1, 2, 3, 5
- [32] Youssef Mroueh, Tom Sercu, and Vaibhava Goel. McGAN: Mean and covariance feature matching GAN. In Doina Precup and Yee Whye Teh, editors, *Proceedings of the 34th International Conference on Machine Learning*, volume 70 of *Proceedings of Machine Learning Research*, pages 2527–2535, International Convention Centre, Sydney, Australia, 06–11 Aug 2017. PMLR. 2, 4
- [33] Tu Nguyen, Trung Le, Hung Vu, and Dinh Phung. Dual discriminator generative adversarial nets. In *Advances in Neural Information Processing Systems*, pages 2670–2680, 2017. 3
- [34] Yao Ni, Dandan Song, Xi Zhang, Hao Wu, and Lejian Liao. Cagan: Consistent adversarial training enhanced gans. In *Proceedings of the Twenty-Seventh International Joint Conference on Artificial Intelligence, IJCAI-18*, pages 2588–2594. International Joint Conferences on Artificial Intelligence Organization, 7 2018. 3, 6
- [35] Sebastian Nowozin, Botond Cseke, and Ryota Tomioka. f-gan: Training generative neural samplers using variational divergence minimization. In *Advances in neural information processing systems*, pages 271–279, 2016. 2

- [36] Augustus Odena, Christopher Olah, and Jonathon Shlens. Conditional image synthesis with auxiliary classifier GANs. In Doina Precup and Yee Whye Teh, editors, *Proceedings of the 34th International Conference on Machine Learning*, volume 70 of *Proceedings of Machine Learning Research*, pages 2642–2651, International Convention Centre, Sydney, Australia, 06–11 Aug 2017. PMLR. [1](#), [2](#), [3](#)
- [37] Scott Reed, Zeynep Akata, Xinchun Yan, Lajanugen Logeswaran, Bernt Schiele, and Honglak Lee. Generative adversarial text to image synthesis. In Maria Florina Balcan and Kilian Q. Weinberger, editors, *Proceedings of The 33rd International Conference on Machine Learning*, volume 48 of *Proceedings of Machine Learning Research*, pages 1060–1069, New York, New York, USA, 20–22 Jun 2016. PMLR. [2](#), [3](#)
- [38] Tim Salimans, Ian Goodfellow, Wojciech Zaremba, Vicki Cheung, Alec Radford, and Xi Chen. Improved techniques for training gans. In *Advances in neural information processing systems*, pages 2234–2242, 2016. [1](#), [2](#), [3](#), [4](#), [6](#)
- [39] Konstantin Shmelkov, Cordelia Schmid, and Karteek Alahari. How good is my gan? In *Proceedings of the European Conference on Computer Vision (ECCV)*, pages 213–229, 2018. [6](#)
- [40] Jost Tobias Springenberg. Unsupervised and Semi-supervised Learning with Categorical Generative Adversarial Networks. *arXiv:1511.06390 [cs, stat]*, Nov. 2015. arXiv: 1511.06390. [3](#)
- [41] Dustin Tran, Rajesh Ranganath, and David Blei. Hierarchical implicit models and likelihood-free variational inference. In *Advances in Neural Information Processing Systems*, pages 5523–5533, 2017. [2](#), [3](#), [5](#)
- [42] Ngoc-Trung Tran, Viet-Hung Tran, Bao-Ngoc Nguyen, Linxiao Yang, and Ngai-Man (Man) Cheung. Self-supervised gan: Analysis and improvement with multi-class minimax game. In H. Wallach, H. Larochelle, A. Beygelzimer, F. d’Alché Buc, E. Fox, and R. Garnett, editors, *Advances in Neural Information Processing Systems 32*, pages 13232–13243. Curran Associates, Inc., 2019. [6](#)
- [43] Yasin Yazıcı, Chuan-Sheng Foo, Stefan Winkler, Kim-Hui Yap, Georgios Piliouras, and Vijay Chandrasekhar. The unusual effectiveness of averaging in GAN training. In *International Conference on Learning Representations*, 2019. [15](#)
- [44] YUI. YU1ut/MixMatch-pytorch, Dec. 2019. original-date: 2019-05-22T03:22:19Z. [14](#)
- [45] Han Zhang, Ian Goodfellow, Dimitris Metaxas, and Augustus Odena. Self-attention generative adversarial networks. In Kamalika Chaudhuri and Ruslan Salakhutdinov, editors, *Proceedings of the 36th International Conference on Machine Learning*, volume 97 of *Proceedings of Machine Learning Research*, pages 7354–7363, Long Beach, California, USA, 09–15 Jun 2019. PMLR. [2](#), [3](#), [5](#)

Appendix A. IS & FID plots

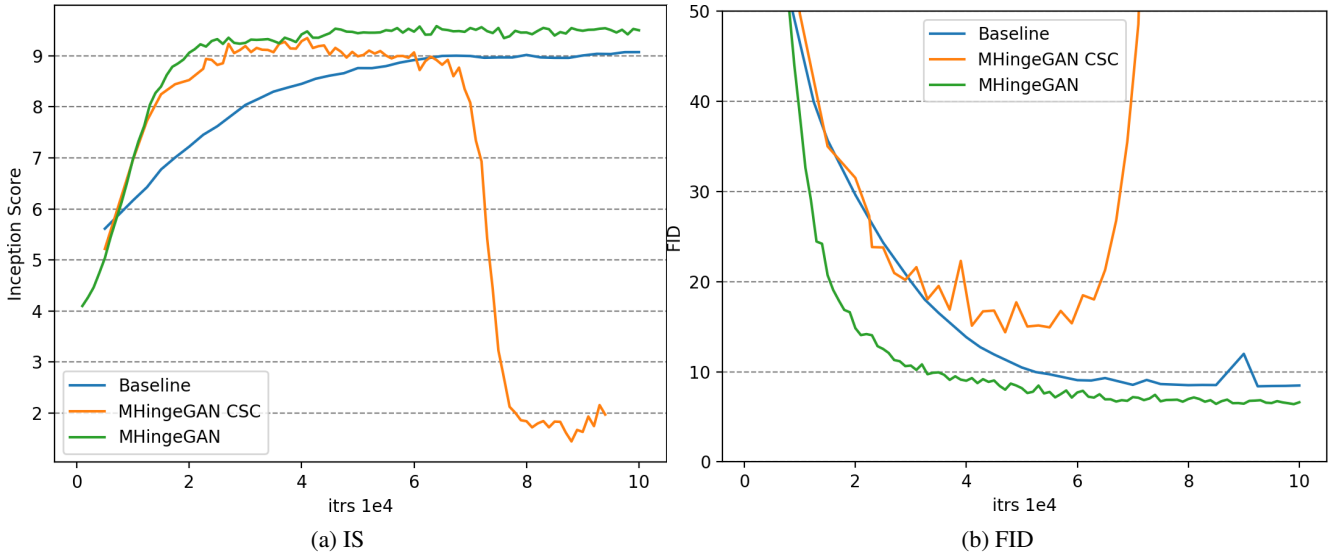


Figure 5: CIFAR10.

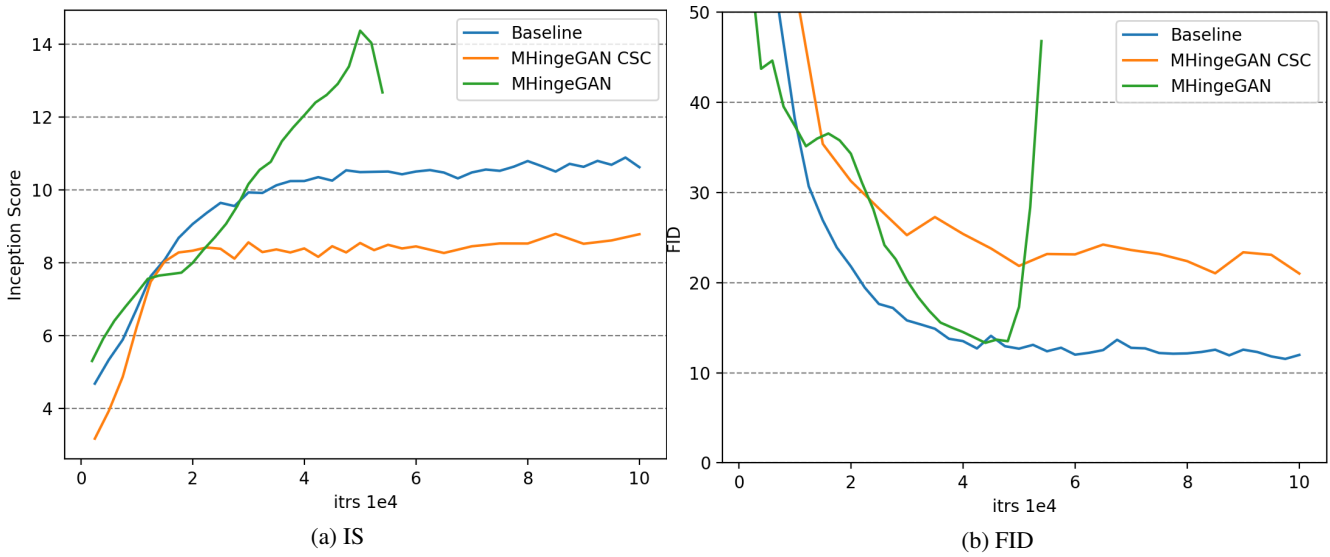


Figure 6: CIFAR100.

Full IS and FID progress for our best model, our baseline, and the better of the two class agnostic ablations/alterations are shown in Figures 5 to 7 for the three datasets we evaluate on.

Appendix B. Network details

The networks we used are shown in Tables 3 to 6. These are the same architectures as used in [30] and elsewhere.

We also note that in training MHingeGAN CSC we found that decreasing the number of discriminator steps per generator step from 4 to 1 and both G and D learning rates to $1e - 4$ after the first 25,000 iterations improved training. This greatly helps to accelerate training, decreasing it earlier led to slower early training. We did not see a similar effect in our baseline.

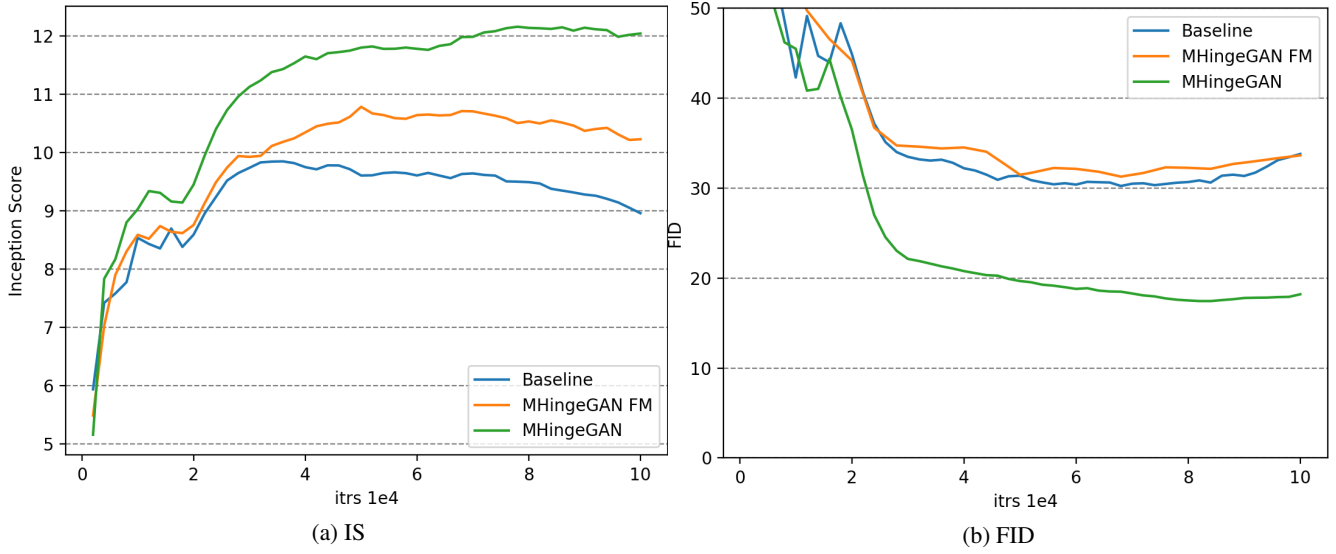


Figure 7: STL10 48x48.

Table 3: 32×32 Generator network.

$z \in \mathbb{R}^{128} \sim \mathcal{N}(0, 0.02)$
dense, $4 \times 4 \times 256$
ResBlock up 256
ResBlock up 256
ResBlock up 256
BN, ReLU, 3×3 conv, Tanh

Table 4: 48×48 Generator network.

$z \in \mathbb{R}^{128} \sim \text{Orthogonal}$
dense, $3 \times 3 \times 1024$
ResBlock up 1024
ResBlock up 512
ResBlock up 256
ResBlock up 128
BN, ReLU, 3×3 conv, Tanh

Appendix C. Random Samples from our best model

See [Figures 8 to 10](#).

Table 5: 32×32 Discriminator/Classifier network.

$x \in \mathbb{R}^{32 \times 32 \times 3}$
ResBlock down 256
ResBlock down 256
ResBlock 256
ResBlock 256
ReLU
Global sum pooling
linear $\rightarrow 1$ or $K + 1$

Table 6: 48×48 Discriminator/Classifier network.

$x \in \mathbb{R}^{48 \times 48 \times 3}$
ResBlock down 64
ResBlock down 128
ResBlock down 256
ResBlock down 512
ResBlock 1024
ReLU
Global sum pooling
linear $\rightarrow 1$ or $K + 1$

Appendix D. Auxiliary network details

For CIFAR10 and CIFAR100 we train a Densenet121 network [22, 26]. These have test set accuracies of 95% and 70% on CIFAR10 and CIFAR100. For STL10 we trained a MixMatch network with 86% test accuracy [5, 44]. We chose these networks because of their availability, and that their test set accuracies are higher than our best C’s accuracy for each dataset.

Appendix E. Additional STL results

Figure 11 shows the four accuracies for STL10 48x48.

E.1. Some 32×32 STL results

There are few comparisons to make in the literature, but our MhingeGAN is also state of the art on STL10 at 32x32 Table 7.



Figure 8: CIFAR10 samples. The classes are: Plane, car, bird, cat, deer, dog, frog, horse, ship, truck.

Table 7: Inception Scores and FIDs for supervised image generation. Methods that are not class conditional are indicated by the †. The best number per column is bold faced.

Method	STL10 32x32	
	IS	FID
Real data	15.67 (± .18)	
Baseline†	9.26 (± .07)	15.95
MHingeGAN SSL	10.12 (± .12)	8.76
MHingeGAN CSC SSL	10.45 (± .09)	12.57
MHingeGAN FM SSL	7.89 (± .11)	-
EMA GAN† [43]	8.39 (± .10)	19.64



(a) Classes 1-25.



(b) Classes 26-50.

Figure 9: CIFAR100 samples. Classes 1-25 are: Apples, aquarium fish, baby, bear, beaver, bed, bee, beetle, bicycle, bottles, bowls, boy, bridge, bus, butterfly, camel, cans, castle, caterpillar, cattle, chair, chimpanzee, clock, cloud, cockroach. Classes 26-50 are: Couch, crab, crocodile, cups, dinosaur, dolphin, elephant, flatfish, forest, fox, girl, hamster, house, kangaroo, keyboard, lamp, lawn-mower, leopard, lion, lizard, lobster, man, maple, motorcycle, mountain.



(a) Classes 51-75.



(b) Classes 76-100.

Figure 10: CIFAR100 samples. Classes 51-75 are: Mouse, mushrooms, oak, oranges, orchids, otter, palm, pears, pickup truck, pine, plain, plates, poppies, porcupine, possum, rabbit, raccoon, ray, road, rocket, roses, sea, seal, shark, shrew. Classes 76-100 are: Skunk, skyscraper, snail, snake, spider, squirrel, streetcar, sunflowers, sweet peppers, table, tank, telephone, television, tiger, tractor, train, trout, tulips, turtle, wardrobe, whale, willow, wolf, woman, worm.

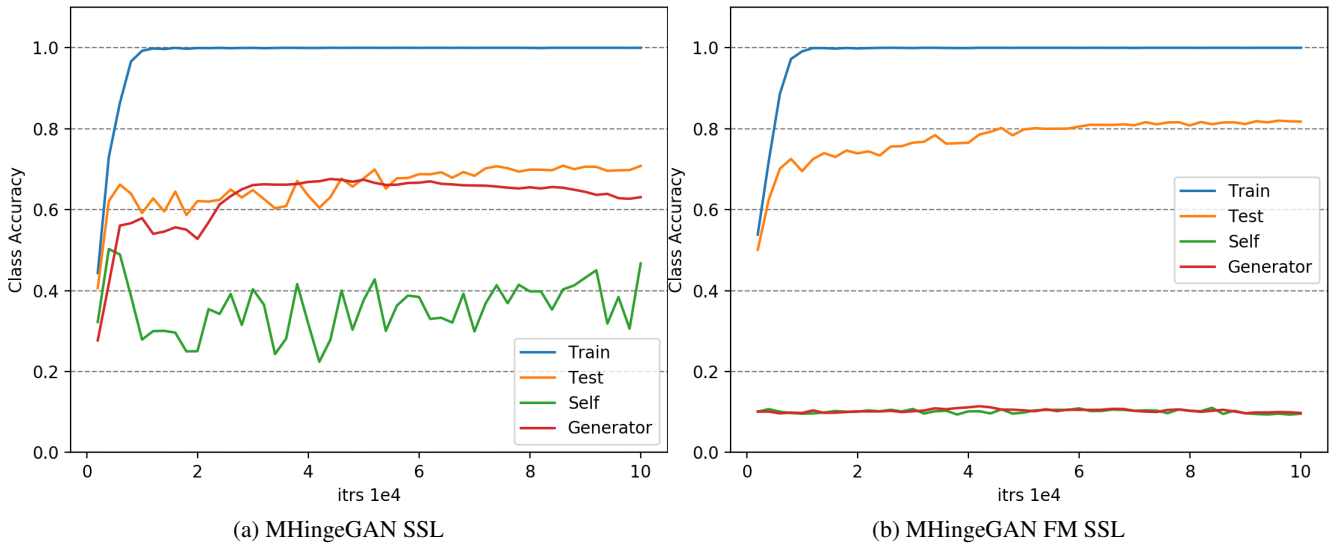


Figure 11: Four accuracies for STL10 48x48.